

Frequency Comb Vernier Spectroscopy for Broadband, High-Resolution, High-Sensitivity Absorption and Dispersion Spectra

Christoph Gohle,^{*} Björn Stein,[†] Albert Schliesser, Thomas Udem, and Theodor W. Hänsch
Max-Planck-Institut für Quantenoptik, Hans-Kopfermann-Straße 1, D-85748 Garching, Germany

(Received 10 June 2007; published 28 December 2007)

A femtosecond frequency comb provides a vast number of equidistantly spaced narrow band laser modes that can be simultaneously tuned and frequency calibrated with 15 digit accuracy. Our Vernier spectrometer utilizes all of these modes in a massively parallel manner to rapidly record both absorption and dispersion spectra with a sensitivity that is provided by a high finesse broadband optical resonator and a resolution that is only limited by the frequency comb line width while keeping the required setup simple.

DOI: [10.1103/PhysRevLett.99.263902](https://doi.org/10.1103/PhysRevLett.99.263902)

PACS numbers: 42.62.Fi, 42.25.Bs, 42.30.Rx, 42.62.Eh

Femtosecond frequency combs [1] provide an equidistant array of narrow linewidth frequencies that can be simultaneously tuned. In this Letter we demonstrate how to employ such a frequency comb to record broadband, high-sensitivity absorption *and* dispersion spectra with potential Hertz resolution in a very short time. The high sensitivity is provided by means of a simple Fabry-Perot resonator that vastly extends the interaction length with the sample under study and has the potential to achieve sensitivities of classical ring-down techniques. The Hertz resolution is provided by an appropriately stabilized frequency comb [2]. As the frequency comb can readily be referenced to a primary frequency standard, the frequency accuracy and reproducibility can be as good as 10^{-15} . To achieve comb mode resolution while keeping the setup simple, the resonator acts as a filter that thins out the frequency comb such that each individual mode can be resolved with the help of a small diffraction grating. The resonator modes are scanned across the frequency comb like a Vernier scale in frequency space. Groups of comb lines that contain the spectroscopic information are streaked on a two-dimensional detector array. In this way a comparatively slow detector such as a charge coupled device (CCD) can be used to acquire a large amount of data in a short time. Similar to a previous method [3] it allows us to determine the dispersive details of the resonator and its contents.

Highly accurate and sensitive detection of complex molecular spectra can have an impact on chemical sensing for, e.g., quick and reliable analysis of compound samples with many different molecules in medical applications. In fundamental physics research this method could also be beneficial. Ultracold molecules, for example, are very interesting candidates for investigating violation of time reversal symmetry [4] or time variation of fundamental constants [5]. Such high precision experiments could naturally benefit from high signal to noise ratio and reproducible calibration. Monitoring many lines simultaneously could help to eliminate systematic effects by using certain lines as probes for environmental conditions. In the past decade a variety of methods were introduced, which ex-

ploit the unique combination of broad bandwidth and high temporal coherence of a frequency comb for sensing and identifying (“fingerprinting”) chemical species [3,6–9]. Some of these techniques take advantage of the temporal coherence by coupling all modes of the frequency comb simultaneously to a dispersion compensated, sensitivity enhancing optical resonator in order to achieve a higher signal-to-noise ratio [7,8]. The spectral resolution is provided by a simple grating spectrometer, ignoring the narrow lines of the frequency comb. Moreover, these methods require accurate dispersion compensation in the resonator, which drastically limits the versatility of this approach. On the other hand, once individual comb modes are resolved, the resolution of a frequency comb spectrometer is only limited by the comb linewidth, which can be on the Hertz level [2]. By combining two spectrally dispersing elements in an arrangement similar to a prism-echelle spectrometer, comb mode resolution over a wide bandwidth has recently been demonstrated [9]. This approach is, however, difficult to combine with a broadband ring-down technique [8] as both methods require a two-dimensional array for detection.

Our frequency comb Vernier spectrometer (Fig. 1) solves these difficulties. It combines the comb mode resolving part of the echelle spectrometer and the sensitivity enhancing high finesse \mathcal{F} resonator into one device. The output of a frequency comb emitting laser has a spectrum containing an equidistant grid of frequencies $\omega_k = \omega_{CE} + k\omega_r$, where ω_r is the pulse repetition frequency of the laser, k is a large integer, and the components are offset from being integer multiples of ω_r by the carrier envelope offset frequency ω_{CE} . This light is sent to the high finesse resonator, which contains the sample under study. It has resonances spaced by its free spectral range $FSR = 2\pi c/nL$, where c is the speed of light in vacuum and n is the effective refractive index. The round-trip length L of the resonator is adjusted such that, if the two scales are lined up, every m th mode from the frequency comb will be resonant with every n th mode of the cavity and transmitted through it. Provided the finesse of the resonator is high enough (i.e., larger than m),

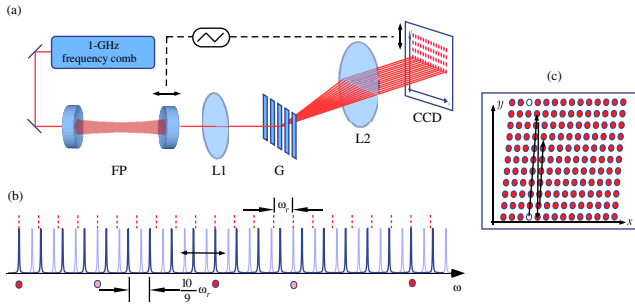


FIG. 1 (color online). (a) General setup: Fabry-Perot (FP) resonator with a scanning mirror; L1, G, L2, spectrograph assembly; CCD, two-dimensional imaging detector, scanned synchronously with FP. (b) Frequency comb (dashed lines) transmission function of the resonator (solid line) from the Vernier. Dots mark transmitted modes for two scan positions. (c) Expected pattern on the detector behind the spectrometer. Arrows mark the order of the frequency comb modes.

the other modes will be strongly suppressed. In this way the modes of the frequency comb and the resonant frequencies of the resonator resemble a Vernier [Fig. 1(b)] with the Vernier ratio $FSR/\omega_r = m/n$ being a cancelled fraction. In our case this is chosen to be $69/68$ ($10/9$ in the figure for clarity). By choosing $m = n + 1$ the interaction length in the resonator is essentially the same as in a matched resonator ($m/n = 1$). Then the frequency comb that is transmitted through the resonator has a spacing of about $m\omega_r/2\pi$, so that for sufficiently large m it can easily be resolved with a very simple and small grating spectrograph. As the length of the resonator is now tuned, the Vernier primarily shifts, bringing the next set of $m\omega_r/2\pi$ spaced comb modes into resonance. After scanning the resonator round-trip length by a wavelength (i.e., one free spectral range), m groups of $m\omega_r/2\pi$ combs have passed by and the situation is as in the beginning, the initial group is transmitted. The only difference is that the Vernier ratio has slightly changed due to the change in resonator length.

A mirror that tilts synchronously with the scanning resonator streaks the light transmitted through it along the axis (y direction) that is perpendicular to the grating dispersion (x direction). A two-dimensional CCD detector is (also synchronized to the scanning) exposed to the output of that spectrometer [in Fig. 1(a) a moving detector is shown for simplicity]. This results in a two-dimensional array of spots on the CCD that can be uniquely ordered into a single frequency axis as shown in Fig. 1(c), very similar to the sorting procedure used in Ref. [9]. We can therefore associate the comb mode frequency $\omega_{i,j} = \omega_{k_0+i+m_j}$ to the spot in row i and column j [counting from an arbitrary spot $(0, 0)$, belonging to frequency ω_{k_0}]. Both the precise value of m and k_0 , and therefore absolute frequency calibration of the data, can easily be determined if there is a sufficiently narrow feature of known (better than ω_r) frequency in the spectrum [e.g., an absorption resonance, open (blue)

spots in Fig. 1(c)]. This feature will repeat itself as the resonator is tuned and the period (in spots) gives the correct value for m . Of course, because the spectrum is only sampled at the comb frequencies, the resolution of a single such pattern is on the order of ω_r and aliasing effects may occur. An essentially arbitrarily high resolution can be achieved by recording a series of spectra with different center frequencies of the frequency comb to fill the gaps.

The spectroscopic information is contained in the brightness and shape of the spots as well as their position. To quantitatively interpret this pattern, we consider a simple steady state model for the signal that is observed on the CCD as a function of frequency (x axis on the CCD) and resonator length (y axis). Assuming the individual comb modes can be well isolated from each other on the CCD image, we can approximate the transmission function in the vicinity of the spot (i, j) as a simple Airy function originating from a single comb mode $\omega_{i,j}$, i.e.,

$$\mathcal{T}_{i,j}(x, y) = \frac{T^2 \delta(\omega(x) - \omega_{i,j})}{1 + r(\omega_{i,j})^2 - 2r(\omega_{i,j}) \cos(\phi(L(y), \omega_{i,j}))}, \quad (1)$$

where r is the round-trip amplitude loss factor $r(\omega) = \sqrt{1 - A(\omega)(1 - T)}$, T the resonator mirror transmission, $A(\omega)$ the absorption of the medium inside the resonator per round-trip, δ the line shape function of the individual frequency comb mode, and $\omega(x)$ and $L(y)$ are appropriate calibration functions of the spectrometer. The line shape δ may be approximated by a Dirac delta function for the most practical purposes. The round-trip phase shift $\phi(L, \omega) = \psi(\omega, L) + L\omega/c$ contains a vacuum contribution $L\omega/c$ and the additional phase shift $\psi(\omega, L)$ due to dispersion of the mirrors and the medium. This Airy function (1) assumes an infinitely large aperture spectrometer and a point source and hence an infinite resolution. With the parameters chosen in this demonstration experiment, however, the actual spot shapes are dominated by the laser beam profile, which can be approximated by a two-dimensional Gaussian of fixed width. The convolution of (1) with this beam profile may be fit to each spot (i, j) in the image to obtain both $A(\omega_{i,j})$ and $\psi(\omega_{i,j})$ up to multiples of 2π , provided y can be calibrated absolutely to the resonator length L [$\omega(x)$ need not be known]. We derived the scaling for $L(y)$ from the fact that $\omega_{i,j}$ and $\omega_{i+m,j-1}$ represent the same frequency, so that the phase shift difference between the two spots needs to be 2π and therefore $L(y_{i+m,j-1}) - L(y_{i,j}) = 2\pi c/\omega_{i,j}$. Here $y_{i,j}$ represents the y position of the peak on the CCD. The dependence of $\psi(L, \omega)$ on the resonator length was neglected in this expression. This is a good assumption as long as the extended medium has a refractive index very close to unity (or has a fixed length). Using this relative length calibration, one may determine $\psi(\omega)$ up to a linear function.

We use a 1 GHz mode locked Ti:sapphire laser with a bandwidth of about 12 THz FWHM centered at 785 nm and an average output power of about 0.5 W as a light source [10]. The spectroscopy resonator consists of broadband dielectric quarter wave stack mirrors, centered at 792 nm and arranged in a bow tie ring cavity configuration. The FSR is about $(69/68)\omega_r$. The two coupling mirrors dominate the resonator loss with their nominal transmission of 0.1%, corresponding to a resonator finesse of $\mathcal{F} = 1000\pi$, which we confirmed by ring-down measurements with the laser operated in the continuous wave mode. One of the coupling mirrors is mounted on a piezoelectric transducer tube for scanning the resonator length. The resonator buildup time of $1 \mu\text{s}$ sets a lower limit of about 3 ms for scanning over one FSR in order to satisfy the steady state approximation that was used in (1). We use a centimeter size 2100 lines per millimeter holographic grating in a 150 mm focal length Czerny-Turner arrangement. The aperture of the grating is fully used to match the resolution of the spectrometer to the pixel size ($5 \mu\text{m}$) of 1000×1200 pixel CCD camera that was used to record the images (WinCAM-D 1M4). The resolution of the spectrometer expected from these parameters is better than 30 GHz at 760 nm. Raw data in the wavelength range from 760 to 770 nm with air inside the resonator obtained in the way described above is shown in Fig. 2. This image was exposed for 9 ms, the time for one scan.

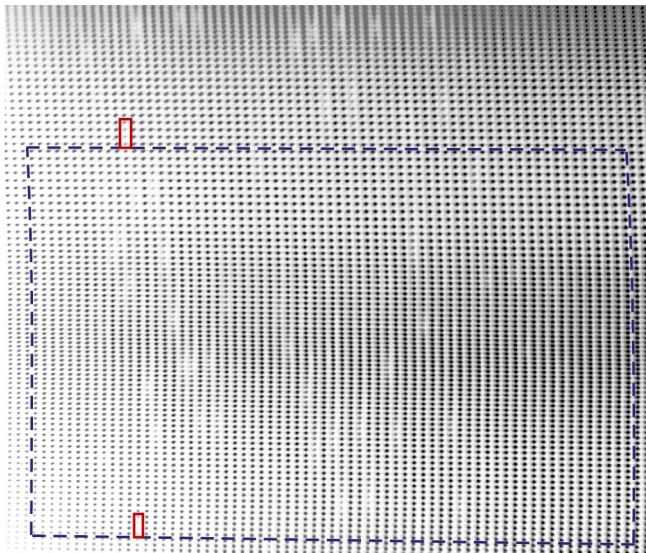


FIG. 2 (color online). Raw data image as seen by the CCD; white corresponds to no light. The horizontal axis is the dispersion axis of the grating and the vertical axis is the scan axis. Weak spots caused by absorption lines in the A bands of O_2 are clearly observed. The period of the pattern in vertical direction indicates the vernier ratio of 69/68 (solid boxes mark exemplary one pattern that was identified). The dashed box marks a unique data set. The varying spot spacing and brightness common to all spot columns originates from a nonlinearity of the scan and is corrected for in the data analysis.

After acquisition, the period of an observed absorption pattern was used to confirm the detuning ratio of the resonator to be 69/68. To obtain brightness values for each spot, a two-dimensional Gaussian was fit to the spot and its integral was used as a brightness value. This is a good approximation to the model (1), as explained above. Because this is the case, the integral was related to the Airy (1) area to obtain an intracavity absorption value. Figure 3(a) shows an absorption spectrum obtained like this after applying a linear filter to the data (see below). A comparison with the high resolution transmission molecular spectroscopic database (HITRAN, [11]) reveals that the absorption feature is caused by the $X^3\Sigma_g^- \rightarrow b^1\Sigma_g^+$ magnetic dipole intercombination transition in molecular oxygen [12]. We used this identification to calibrate the offset frequency ω_{CE} , which was not measured independently in this demonstration. Note that our measurement perfectly agrees in frequency scale, amplitude, and linewidth with the database values (Fig. 3).

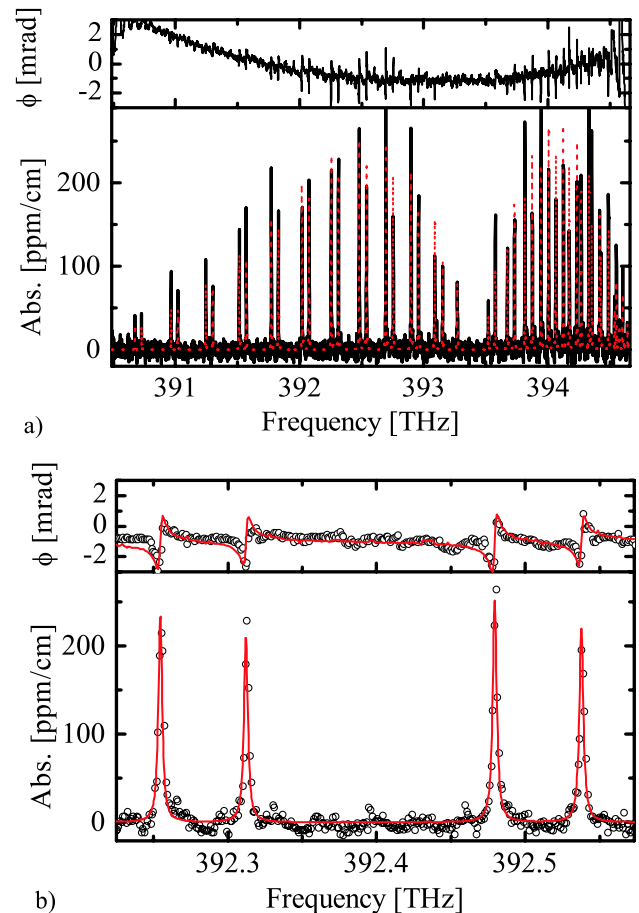


FIG. 3 (color online). (a) Spectrum extracted from the raw data (solid line) and HITRAN [11] database values (dashed red line). The phase shows a global positive second-order dispersion of the resonator and spikes at the resonances. (b) Zoom of the data set, highlighting the excellent agreement between our data (circles) and the HITRAN database (red line).

One strength of the method is to provide both amplitude and phase information about the sample, the latter of which is also shown in Fig. 3. This (round-trip) phase spectrum has a suitable linear function subtracted in order to make the dispersion more easily seen. It shows a global second-order dispersion, as expected from the dielectric mirrors that were used at the blue end of the mirrors' reflectance. On top of that local dispersive features are seen, which agree, in position and amplitude, with the expected dispersive features of the O₂ resonances. The phase sensitivity with the current implementation is not specifically high, as the Airy pattern is not resolved by the spectrometer so that the phase information is degraded.

By evaluating the rms absorption noise level at positions where no signal is detected, we estimate the absorption sensitivity of the method for a single frequency to be $5 \times 10^{-6} \text{ cm}^{-1}$ for a single image taken within 10 ms. This is about a factor of 500 above the shot noise limit ($\approx 1 \mu\text{W}$ power per mode, average transmission during the scan $\pi/2\mathcal{F}$, sensitivity enhanced by $\mathcal{F}/2\pi$), due to technical noise. For instance, mechanical noise can render the cavity scan nonlinear in time. This leads to varying integration times and positions for the individual comb modes and adds noise to the extracted absorption and dispersion information. However, because the scan position is the same for the same vertical position on the camera, such distortions of the pattern are common to each spot column. An obvious example is the higher spot density in the vertical center of Fig. 2. An appropriate linear filter was used to effectively reduce this type of noise. Such a filter will of course also reject real structure with a period of the length of one column. Such a case can, however, easily be tested for by changing the detuning and therefore the column length.

In conclusion, we have presented a simple method that provides comb line resolution over a bandwidth of more than 4 THz, which should be easily extensible to 40 THz by packing the spot pattern more tightly. Simultaneously the sensitivity is better than $10^{-6} \text{ cm}^{-1} \text{ Hz}^{-1/2}$ per mode, which was achieved in an interaction length of 29 cm only using a moderately high \mathcal{F} optical resonator. The method can be made equivalent to a ring-down method by increasing the scan speed and replacing (1) with an appropriate non-steady-state version [13] in order to get into a real ring-down regime. Then, if the streak speed is chosen appropriately so that the ring-down wave form can be seen, the decay time may be separated from the influence of technical noise. In addition to ring-down methods it also provides dispersion information with a potential accuracy equivalent or exceeding the one presented in [3]. Because of the scanning resonator approach, it is not necessary to accurately control intracavity dispersion, which in other methods results in a reduced transmission or even spurious signals. The price that has to be paid for these advantages compared to matched resonators is that the average power transmission through the resonator is

$\pi/2\mathcal{F}$ so that the shot noise limited absorption sensitivity only scales as the square root of the finesse instead of the finesse itself. Yet our method is fast. A single acquisition takes only about 10 ms giving 4000 data points (4 THz with a resolution of 1 GHz). With little optimization, one can easily obtain 20 000–40 000 spots on a megapixel CCD (the only requirement being that the spots are well separated). The resolution of the scheme is essentially unlimited (hertz level, due to potential laser linewidth). This is in contrast to customary Vernier spectroscopy techniques (e.g., [14]), using a noncoherent broadband source in conjunction with multiple etalons instead of a frequency comb. These can hardly exceed a bandwidth/resolution ratio of 10^6 while our technique promises values exceeding 10^{12} . And it can, at any time, be referenced to a primary frequency standard, giving a frequency reproducibility and accuracy of 10^{-15} (subhertz level), which is limited by the primary standard only. The potentially high resolution naturally suggests the application of the demonstrated technique to some kind of cavity enhanced nonlinear Doppler free spectroscopy [15].

This research was supported by the DFG cluster of excellence Munich Centre for Advanced Photonics.

*cgohle@few.vu.nl

†Current address: Physikalisch-Technische Bundesanstalt, Braunschweig, Germany.

- [1] Th. Udem, R. Holzwarth, and T.W. Hänsch, *Nature (London)* **416**, 233 (2002).
- [2] A. Bartels, C.W. Oates, L. Hollberg, and S.A. Diddams, *Opt. Lett.* **29**, 1081 (2004).
- [3] A. Schliesser, C. Gohle, Th. Udem, and T.W. Hänsch, *Opt. Express* **14**, 5975 (2006).
- [4] J.J. Hudson, B.E. Sauer, M.R. Tarbutt, and E.A. Hinds, *Phys. Rev. Lett.* **89**, 023003 (2002).
- [5] E. Reinhold, R. Buning, U. Hollenstein, A. Ivanchik, P. Petitjean, and W. Ubachs, *Phys. Rev. Lett.* **96**, 151101 (2006).
- [6] F. Keilmann, C. Gohle, and R. Holzwarth, *Opt. Lett.* **29**, 1542 (2004).
- [7] T. Gherman and D. Romanini, *Opt. Express* **10**, 1033 (2002).
- [8] M.J. Thorpe, K.D. Moll, R.J. Jones, B. Safdi, and J. Ye, *Science* **311**, 1595 (2006).
- [9] S.A. Diddams, L. Hollberg, and V. Mbele, *Nature (London)* **445**, 627 (2007).
- [10] A. Bartels, T. Dekorsy, and H. Kurz, *Opt. Lett.* **24**, 996 (1999).
- [11] L.S. Rothman *et al.*, *J. Quant. Spectrosc. Radiat. Transfer* **96**, 139 (2005).
- [12] P.H. Krupenie, *J. Phys. Chem. Ref. Data* **1**, 423 (1972).
- [13] K. An, C. Yang, R.R. Dasari, and M.S. Feld, *Opt. Lett.* **20**, 1068 (1995).
- [14] J.E. Mack, D.P. McNutt, F.L. Roesler, and R. Chabbal, *Appl. Opt.* **2**, 873 (1963).
- [15] L.S. Ma and J.L. Hall, *IEEE J. Quantum Electron.* **26**, 2006 (1990).